SICE Annual Conference 2011
September 13-18, 2011, Waseda University, Tokyo, Japan

Motion Representation of Walking/Slipping/Turnover for Humanoid Robot by Newton-Euler Method

Tomohide Maeba[1], Geng Wang[1], Fujia Yu[1], Mamoru Minami[1] and Akira Yanou[1]

[1]Graduate School of Natural Science and Technology, Okayama University, Okayama, Japan
(Tel: +81-86-251-8924; E-mail: maeba@suri.sys.okayama-u.ac.jp)

Abstract: This paper proposes a formulation of dynamical equation of bipedal walking model of humanoid robot with foot by Newton-Euler Method well-known in robotics field as a calculation scheme of dynamics, which can describe a dynamical effect of foot's slipping without any approximation. This formulation including kicking torque of foot inevitably and naturally generates sequential variety in dynamical walking gait pattern—derived from orders of detaching/landing sequences—which has been ignored in case of round-foot or point-foot model.

Keywords: Bipedal walking, Geometric constraint condition, Newton-Euler method.

1. INTRODUCTION

Human beings have acquired an ability of stable bipedal walking in evolving repetition so far. From a view point of making a stable controller for the bipedal walking based on knowledge of control theory, it looks like to be not easy because of the dynamics with high nonlinearity and coupled interactions between state variables with high dimensions.

Therefore how to simplify the complicated walking dynamics to help construct stable walking controller has been studied intensively. ZMP-based static walking is one of potential approaches, which has been proved to be a realistic control strategy to realize stable walking of actual biped robot, since it can guarantee that the robots can keep standing by retaining the zero moment point within the convex hull of supporting area [1, 2]. Honda's humanoid robot has achieved static walking in real world by referring a trajectory examined intensively to have the robot's ZMP located inside the supporting area [3].

Instead of the ZMP, another approaches that put the importance on keeping the robot's walking trajectories inside of a basin of attraction [4]-[6] including a method referring limit cycle to determine input torque [7].

Avoiding complications in dealing directly with true dynamics without approximation, inverted pendulum has been used frequently for making a stable controller [8]-[12], simplifying the calculations to determine input torque. Further linear approximation of the humanoid robot into simple inverted pendulum enables researchers to aim at realizing stable gait through well-known control strategy, i.e., Model Predictive Control, changing the problem of stable walking into optimization of an objective function from current time to prediction horizon [13]-[15]. These previous discussions are all based on simplified bipedal model, which avoided to discuss the effect of foot and slipping motion existing usually in real world.

Contrarily to the above the references using simplified bipedal model, a research [16] has clearly pointed out that the effect of foot derives varieties of the walking gate, i.e., whether a heel lands floor faster than toe or vice versa depends fully on the walking dynamics and ground's shape, which could not be predetermined. And that what, the authors think, is more important is that the dimension of the dynamical equation will change depending on the walking gate's varieties. When the Foot's underside surface contacts flatly the ground without slipping, the foot does not move of course, having the foot excluded from the dynamical equation. However given that as an example, the foot should start slipping or the heel be detached from the ground while its toe being contacting, a new state variable describing slipping or rotating would emerge, resulting in an increase of a number of state variables. On the other hand, landing of the heel or the toe of the lifting leg in the air to the ground makes a geometrical contact, i.e., algebraic constraint should reduce the dimension of the dynamical model [17, 18]. This kind of dynamics with the dimension number of state variables being changed by the result of its dynamical time transitions are out of the arena of control theory that discusses how to control a system with fixed states' number.

Our research has begun from such view point of [16] as aiming at describing gait dynamics as correctly as possible, including slipping of the foot on the ground. This kind of slip can be represented by using the dynamics proposed in [19], which can model constrained motion with friction. However, our modeling approach differs from [16] in that it utilizes Lagrangian Method, instead of that we adopted Newton-Euler [NE] Method [20] that calculates all links' dynamics with full dynamical freedom of six (3 for position, 3 for rotation). Furthermore the NE Method helps to include easily the slipping freedom of foot into the description of the dynamics, as has been written in this paper, and also being useful for solving forward dynamics calculations [21].

2. DYNAMICAL HUMANOID MODEL

2.1 Model of Single-foot Standing

Humanoid robot standing on one supporting foot can be modeled as a serial link manipulator having a ramification of torso and floating leg split from standing leg. A merit to formulate an equation of motion of serial-link manipulator by NE Method is that we need not to differ-

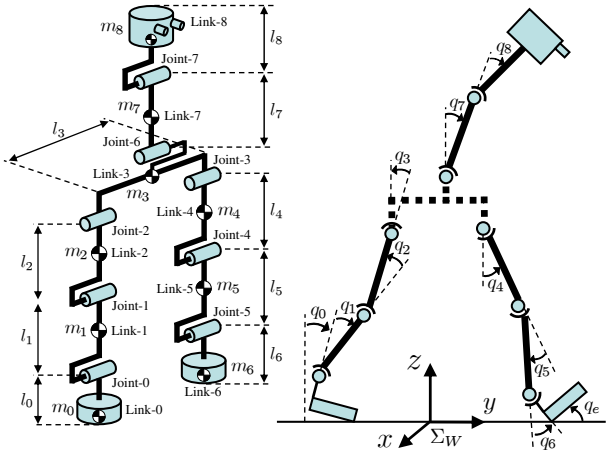

Fig. 1 Model of humanoid robot

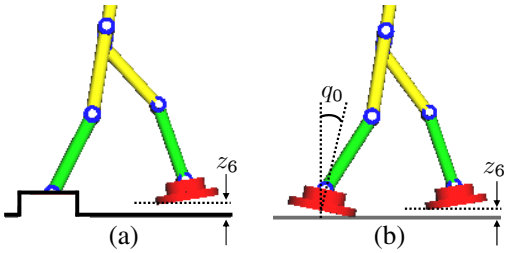

Fig. 2 Phase (I) and (I′)

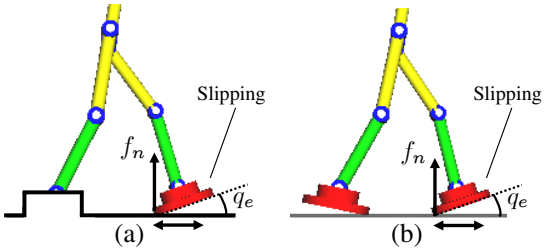

Fig. 3 Phase (II) and (II′)

entiate a kinetic energy like Lagrange Method, where the calculation of partial differentiation explosively swells as the number of links increase, which should be avoided especially when we make a dynamical model of humanoid robot with many links and freedoms of motion. In this paper, we discuss the motion in sagittal plane as a biped robot and whose definition of joint angle is depicted in Fig. 1. Though its motion is restricted in sagittal plane, it has fertile dynamics since the robot has flat-sole feet and kicking torque, then this feature generates varieties of walking gait sequences, which does not appear in case of round-foot and point-foot.

Avoiding the partial differentiations, and following the formulation by NE Method, we first have to calculate relations of positions, velocities and accelerations between links as forward kinematics procedures from bottom link to top link [20]. While the two links—a torso of 7-th link, and left leg of 4-th link—are ramified from waist of 3-rd link, as shown Fig. 1, the acceleration of the center of gravity $\ddot{\boldsymbol{s}}_i, i = 4, 7$ of 4-th and 7-th links based on world coordinates $\boldsymbol{\Sigma}_W$, can be calculated based on the acceleration of 3-rd link by:

$$\ddot{\boldsymbol{s}}_i = \ddot{\boldsymbol{p}}_3 + \dot{\boldsymbol{\omega}}_i \times {}^i\hat{\boldsymbol{s}}_i + \boldsymbol{\omega}_i \times (\boldsymbol{\omega}_i \times {}^i\hat{\boldsymbol{s}}_i). \tag{1}$$

Here, ${}^i\hat{\boldsymbol{s}}_i$ means gravity center position of the i-th link based on coordinates $\boldsymbol{\Sigma}_i$ fixed at i-th link, and 3×3 matrix $\boldsymbol{R}_i$ represents orientation matrix of i-th link based on $\boldsymbol{\Sigma}_W$. $\ddot{\boldsymbol{p}}_3$ represents acceleration at the origin of $\boldsymbol{\Sigma}_i$ and $\boldsymbol{\omega}_i$ is angular velocity of the i-th link. When there is no prefix letter at the top left corner, it means the vector or the matrix is expressed in the world frame Σ_W.

After the above forward kinematic calculation has been done, contrarily backward force and torque transferring calculation is the next from top to base link. Newton equation of the i-th link rigid body and Euler equation are represented by Eqs. (2), (3) below when m_i, $\boldsymbol{I}_i$ and ${}^i\hat{\boldsymbol{p}}_{i+1}$ are defined as mass of i-th link, inertia tensor of i-th link and position vector from the origin of i-th link to the one of $(i+1)$-th. The rotational motion equations of motor joints are obtained as Eq. (4) by making inner product of induced torque onto the i-th link's rotational axis unit vector $\boldsymbol{e}_{zi}$.

$$ {}^i\boldsymbol{f}_i = {}^i\boldsymbol{R}_{i+1}\,{}^{i+1}\boldsymbol{f}_{i+1} + m_i\,{}^i\ddot{\boldsymbol{s}}_i, \tag{2}$$

$$ \begin{aligned} {}^i\boldsymbol{n}_i = {}& {}^i\boldsymbol{R}_{i+1}\,{}^{i+1}\boldsymbol{f}_{i+1} + \boldsymbol{I}_i\,{}^i\dot{\boldsymbol{\omega}}_i + {}^i\boldsymbol{\omega}_i \times (\boldsymbol{I}_i\,{}^i\boldsymbol{\omega}_i) \\ & + {}^i\hat{\boldsymbol{s}}_i \times (m_i\,{}^i\ddot{\boldsymbol{s}}_i) + {}^i\hat{\boldsymbol{p}}_{i+1} \times ({}^i\boldsymbol{R}_{i+1}\,{}^{i+1}\boldsymbol{f}_{i+1}), \end{aligned} \tag{3}$$

$$ \tau_i = (\boldsymbol{e}_{zi})^T\,{}^i\boldsymbol{n}_i. \tag{4}$$

Since force and torque of 4-th and 7-th links are exerted on 3-rd link, effects influence onto 3-rd link as:

$$ {}^3\boldsymbol{f}_3 = {}^3\boldsymbol{R}_4\,{}^4\boldsymbol{f}_4 + {}^3\boldsymbol{R}_7\,{}^7\boldsymbol{f}_7 + m_3\,{}^3\ddot{\boldsymbol{s}}_3, \tag{5}$$

$$ \begin{aligned} {}^3\boldsymbol{n}_3 = {}& {}^3\boldsymbol{R}_4\,{}^4\boldsymbol{n}_4 + {}^3\boldsymbol{R}_7\,{}^7\boldsymbol{n}_7 + \boldsymbol{I}_3\,{}^3\dot{\boldsymbol{\omega}}_3 + {}^3\boldsymbol{\omega}_3 \times (\boldsymbol{I}_3\,{}^3\boldsymbol{\omega}_3) \\ & + {}^3\hat{\boldsymbol{s}}_3 \times (m_3\,{}^3\ddot{\boldsymbol{s}}_3) + {}^3\hat{\boldsymbol{p}}_4 \times ({}^3\boldsymbol{R}_4\,{}^4\boldsymbol{f}_4) \\ & + {}^3\hat{\boldsymbol{p}}_7 \times ({}^3\boldsymbol{R}_7\,{}^3\boldsymbol{f}_7), \end{aligned} \tag{6}$$

$$ \tau_3 = (\boldsymbol{e}_{z3})^T\,{}^3\boldsymbol{n}_3. \tag{7}$$

Eq. (7) is the dynamical equation of 3-rd link. The equation of motion of other serial links without ramification as shown Eq. (4) can be derived by known inverse dynamical calculation procedures [20] in case of $i = 1, 2, 4, \cdots, 8$. Finally, we can get the equation of motion with one leg standing as:

$$\boldsymbol{M}(\boldsymbol{q})\ddot{\boldsymbol{q}} + \boldsymbol{h}(\boldsymbol{q}, \dot{\boldsymbol{q}}) + \boldsymbol{g}(\boldsymbol{q}) + \boldsymbol{D}\dot{\boldsymbol{q}} = \boldsymbol{\tau}, \tag{8}$$

where, joint angle $\boldsymbol{q} = [q_1, q_2, \cdots, q_8]^T$ and the supporting foot is assumed to be without slipping. $\boldsymbol{M}$ is inertia matrix, $\boldsymbol{h}$ and $\boldsymbol{g}$ are vectors which indicate Coriolis force, centrifugal force and gravity, $\boldsymbol{D} = diag[d_0, d_1, \cdots, d_7]$ is matrix which indicates coefficients of joints' viscous friction and $\boldsymbol{\tau}$ is input torque. This phase of walking pattern is depicted in Fig. 2 (a). When the heel of the standing foot should detach from the ground before the lifting foot contacts to the ground as shown in Fig. 2 (b), the state variable for the foot's angle q_0 be added to $\boldsymbol{q}$, thus $\boldsymbol{q} = [q_0, q_1, \cdots, q_8]^T$, but $\tau_0 = 0$ since the toe cannot exert any torque.

2.2 Model with Single Contacting Constraints

Given a lifting foot contacts with a ground while keeping Phase (I), the Phase (II) appears like Fig. 3 (a) with

the forefoot's z-axis position being constrained by the ground. This constraint is represented by Eq. (9), where $\boldsymbol{r}(\boldsymbol{q})$ represents forefoot's position in $\boldsymbol{\Sigma}_W$.

$$C_1(\boldsymbol{r}(\boldsymbol{q})) = 0 \tag{9}$$

With state variables of Eq. (8) being given $\boldsymbol{q} = [q_1, q_2, \cdots, q_8]^T$ and combining it with Eq. (9), the Phase (II) in Fig. 3 (a) can be modeled, where the forefoot's motion in y-axis direction in $\boldsymbol{\Sigma}_W$, i.e., walking direction has a degree of motion that means the forefoot can slip forward or backward depending on the foot's velocity in y-axis before touching down to the ground. Translate condition from Phase (I) to (II), and other conditions will be discussed in section IV. It is a common sense that (i) the reaction force f_n and friction force of the forefoot f_t are orthogonal and (ii) f_t is proportional to f_n, i.e., $f_t = Kf_n$ (K is constant scalar). When the forefoot does not slip, f_t acts as static friction. On the other hand, when the foot slips, it acts as dynamic friction. Then the equation of motion with single constraint can be expressed as:

$$\begin{aligned}\boldsymbol{M}(\boldsymbol{q})\ddot{\boldsymbol{q}} + \boldsymbol{h}(\boldsymbol{q}, \dot{\boldsymbol{q}}) + \boldsymbol{g}(\boldsymbol{q}) + \boldsymbol{D}\dot{\boldsymbol{q}} \\ = \boldsymbol{\tau} + \boldsymbol{j}_c^T f_n - \boldsymbol{j}_t^T f_t \\ = \boldsymbol{\tau} + (\boldsymbol{j}_c^T - \boldsymbol{j}_t^T K) f_n,\end{aligned} \tag{10}$$

where $\boldsymbol{j}_c$ and $\boldsymbol{j}_t$ are defined as:

$$\boldsymbol{j}_c^T = \left(\frac{\partial C_1}{\partial \boldsymbol{q}^T}\right)^T \left(1 / \left\| \frac{\partial C_1}{\partial \boldsymbol{r}^T} \right\|\right), \quad \boldsymbol{j}_t^T = \left(\frac{\partial \boldsymbol{r}}{\partial \boldsymbol{q}^T}\right)^T \frac{\dot{\boldsymbol{r}}}{\|\dot{\boldsymbol{r}}\|}. \tag{11}$$

Moreover, Eq. (9) are differentiated by time two times, then we can derive the constraint condition of $\ddot{\boldsymbol{q}}$.

$$\left(\frac{\partial C_1}{\partial \boldsymbol{q}^T}\right) \ddot{\boldsymbol{q}} + \dot{\boldsymbol{q}}^T \left\{ \frac{\partial}{\partial \boldsymbol{q}} \left(\frac{\partial C_1}{\partial \boldsymbol{q}^T}\right) \right\} \dot{\boldsymbol{q}} = 0 \tag{12}$$

The $\ddot{\boldsymbol{q}}$ in Eq. (10) and Eq. (12) should be identical so the time solution of Eq. (12) be under the constraint of Eq. (9). Then the following simultaneous equation of $\ddot{\boldsymbol{q}}$ and the f_n have to be maintained during the contacting period of the motion. Here, the f_n is decided dependently to make the $\ddot{\boldsymbol{q}}$ in Eq. (10) and Eq. (12) to be identical.

$$\begin{aligned}&\begin{bmatrix} \boldsymbol{M}(\boldsymbol{q}) & -(\boldsymbol{j}_c^T - \boldsymbol{j}_t^T K) \\ \dfrac{\partial C_1}{\partial \boldsymbol{q}^T} & 0 \end{bmatrix} \begin{bmatrix} \ddot{\boldsymbol{q}} \\ f_n \end{bmatrix} \\ &= \begin{bmatrix} \boldsymbol{\tau} - \boldsymbol{h}(\boldsymbol{q}, \dot{\boldsymbol{q}}) - \boldsymbol{g}(\boldsymbol{q}) - \boldsymbol{D}\dot{\boldsymbol{q}} \\ -\dot{\boldsymbol{q}}^T \left\{ \dfrac{\partial}{\partial \boldsymbol{q}} \left(\dfrac{\partial C_1}{\partial \boldsymbol{q}^T} \right) \right\} \dot{\boldsymbol{q}} \end{bmatrix}\end{aligned} \tag{13}$$

When the heel of the hind leg should detach from the ground while forefoot's heel contacting to the ground as shown Fig. 3 (b), the state variable for the foot's angle q_0 be added to $\boldsymbol{q}$, increasing to $\boldsymbol{q} = [q_0, q_1, \cdots, q_8]^T$. With the including q_0 as $\boldsymbol{q} = [q_0, q_1, \cdots, q_8]^T$, the equation of motion Eq. (13) represents the motion in Fig. 3 (b), Phase (II′).

Moreover, Fig. 4 indicates a situation that the forefoot is stationary and rear-foot's toe is contacting. In this

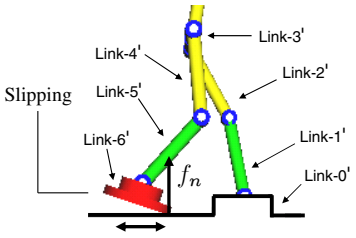

Fig. 4 Phase (IV)

phase, the tiptoe of rear-foot is point-contacting. Since this situation can be thought to be the same as the Phase (II), which means that the walking phases are completely reversible about fore and hind foot, we can represent this Phase (IV) by using Eq. (13)

2.3 Model with Plural Contacting Constraints

When the forefoot's sole surface contacts to the ground as shown Fig 5 (a), another constraint emerges besides the z-axis constraint C_1 defined by Eq. (9) so forefoot's angle has to be kept as zero, that is $C_2(\boldsymbol{r}(\boldsymbol{q})) = 0$, then the plural constraints are

$$\boldsymbol{C}(\boldsymbol{r}(\boldsymbol{q})) = \begin{bmatrix} C_1(\boldsymbol{r}(\boldsymbol{q})) \\ C_2(\boldsymbol{r}(\boldsymbol{q})) \end{bmatrix} = \boldsymbol{0}, \tag{14}$$

where in this case $C_2(\boldsymbol{r}(\boldsymbol{q})) = q_e = q_1 + q_2 + \cdots + q_6 = 0$. Then, robot's equation of motion with external forces f_n and τ_n corresponding to C_1 and C_2 can be derived by the same procedures as Eq. (10):

$$\begin{aligned}\boldsymbol{M}(\boldsymbol{q})\ddot{\boldsymbol{q}} + \boldsymbol{h}(\boldsymbol{q}, \dot{\boldsymbol{q}}) + \boldsymbol{g}(\boldsymbol{q}) + \boldsymbol{D}\dot{\boldsymbol{q}} \\ = \boldsymbol{\tau} + (\boldsymbol{j}_c^T - \boldsymbol{j}_t^T K) f_n + \boldsymbol{j}_r^T \tau_n,\end{aligned} \tag{15}$$

where $\boldsymbol{j}_r$ is

$$\boldsymbol{j}_r^T = \left(\frac{\partial C_2}{\partial \boldsymbol{q}^T}\right)^T \left(1 / \left\| \frac{\partial C_2}{\partial \boldsymbol{q}^T} \right\|\right). \tag{16}$$

Differentiating by time two times Eq. (14), and combining it with Eq. (15), we get,

$$\begin{aligned}&\begin{bmatrix} \boldsymbol{M}(\boldsymbol{q}) & -(\boldsymbol{j}_c^T - \boldsymbol{j}_t^T K) & -\boldsymbol{j}_r^T \\ \partial C_1/\partial \boldsymbol{q}^T & 0 & 0 \\ \partial C_2/\partial \boldsymbol{q}^T & 0 & 0 \end{bmatrix} \begin{bmatrix} \ddot{\boldsymbol{q}} \\ f_n \\ \tau_n \end{bmatrix} \\ &= \begin{bmatrix} \boldsymbol{\tau} - \boldsymbol{h}(\boldsymbol{q}, \dot{\boldsymbol{q}}) - \boldsymbol{g}(\boldsymbol{q}) - \boldsymbol{D}\dot{\boldsymbol{q}} \\ -\dot{\boldsymbol{q}}^T \left\{ \dfrac{\partial}{\partial \boldsymbol{q}} \left(\dfrac{\partial C_1}{\partial \boldsymbol{q}^T} \right) \right\} \dot{\boldsymbol{q}} \\ -\dot{\boldsymbol{q}}^T \left\{ \dfrac{\partial}{\partial \boldsymbol{q}} \left(\dfrac{\partial C_2}{\partial \boldsymbol{q}^T} \right) \right\} \dot{\boldsymbol{q}} \end{bmatrix}.\end{aligned} \tag{17}$$

3. WALKING GAIT TRANSITION

Fig. 6 denotes bipedal walking gait transition. In the phase that has ramification, the gait is switched to next phase in case of auxiliary written switching condition being satisfied. What the authors want to emphasize here is that the varieties of this transition completely depend on the solution of dynamics shown as Eqs. (8), (13), (17).

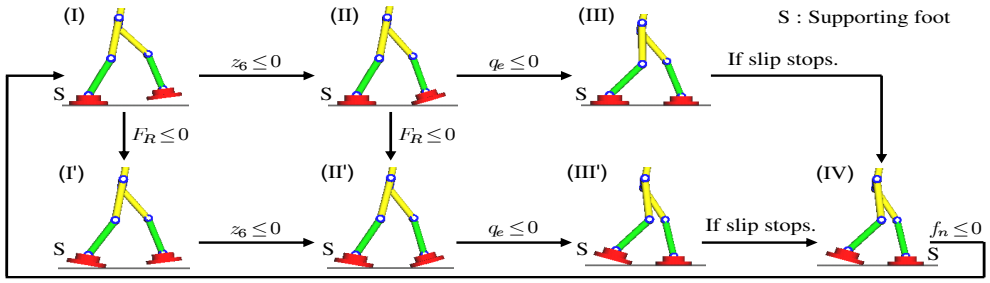

Fig. 6 Phase and gait transition

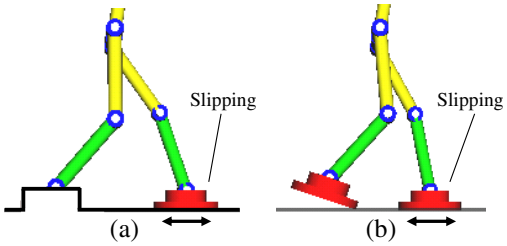

Fig. 5 Phase (III) and (III′)

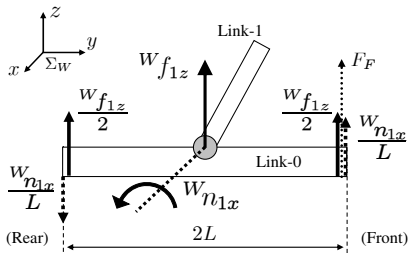

Fig. 7 Force and moment act on Link-0

Therefore, we cannot predetermine the walking gaits pattern, contrarily it will be depended on the initial conditions of the robot, input torque, the shape of the ground and so on.

3.1 Transition from (I) to (I′) or from (II) to (II′)

A condition that a heel of the rear-foot detaches from the ground in Phase (I) or (II) is discussed here. For this judge, force ${}^1\boldsymbol{f}_1$ and moment ${}^1\boldsymbol{n}_1$ derived from Eqs. (2), (3) ($i = 1$) are used. Firstly, reference coordinate of ${}^1\boldsymbol{f}_1$ and ${}^1\boldsymbol{n}_1$ is converted from Σ_1 to Σ_W by ${}^W\boldsymbol{f}_1 = {}^W\boldsymbol{R}_1 {}^1\boldsymbol{f}_1$ and ${}^W\boldsymbol{n}_1 = {}^W\boldsymbol{R}_1 {}^1\boldsymbol{n}_1$. Then, projection to z-axis of ${}^W\boldsymbol{f}_1$ and projection to x-axis of ${}^W\boldsymbol{n}_1$ are derived by using unit vector $\boldsymbol{e}_x$ and $\boldsymbol{e}_z$.

$$ {}^W f_{1z} = (\boldsymbol{e}_z)^T {}^W\boldsymbol{f}_1, \quad {}^W n_{1x} = (\boldsymbol{e}_x)^T {}^W\boldsymbol{n}_1 \tag{18} $$

Given that the foot's contacting points are to be two points of tip and heel, ${}^W f_{1z}$ and ${}^W n_{1x}$ are converted to two reaction force exerting from the ground to the tiptoe and heel of Link-0 as shown Fig. 7. Here, when resultant forces that act on rear/front of Link-0 are defined as F_R and F_F respectively, we can get two equations below.

$$ F_R = \frac{{}^W f_{1z}}{2} - \frac{{}^W n_{1x}}{L}, \quad F_F = \frac{{}^W f_{1z}}{2} + \frac{{}^W n_{1x}}{L} \tag{19} $$

Thus, when value of F_R becomes negative, Link-0 begins to rotate around the tiptoe, which means the heel detaches from the ground. For this reason, an inequality $F_R < 0$ is a condition expression for switching.

3.2 Transition from (I) to (II) and from (I′) to (II′)

This transition means that the heel of the forefoot (Link-6) attaches to the ground in Phase (I) or (I′). Therefore, when z-axis of the heel is defined as z_6 shown as Fig. 2, switching condition is $z_6 \leq 0$.

3.3 Transition from (II) to (III) and from (II′) to (III′)

This change of phase means that the tiptoe of the forefoot (Link-6) attaches to the ground in Phase (II) or (II′). By using q_e in Fig. 3, switching condition is $q_e \leq 0$.

During the transition in previous subsection and this subsection, we consider collision between foot and ground by using the method introduced in [16]. By integration of motion equation with constraint, equation of striking moment can be obtained.

$$ \boldsymbol{M}(\boldsymbol{q})\dot{\boldsymbol{q}}^+ = \boldsymbol{M}(\boldsymbol{q})\dot{\boldsymbol{q}}^- + \boldsymbol{j}_c^T I_c \tag{20} $$

$$ \boldsymbol{M}(\boldsymbol{q})\dot{\boldsymbol{q}}^+ = \boldsymbol{M}(\boldsymbol{q})\dot{\boldsymbol{q}}^- + \boldsymbol{j}_r^T I_r \tag{21} $$

Eq. (20) describes the collision of lateral motion in z-axis of Σ_W between the heel and the ground, and Eq. (21) describes the collision of rotational motion around x-axis between the tiptoe and the ground. $\dot{\boldsymbol{q}}^+$ and $\dot{\boldsymbol{q}}^-$ are angular velocity after and before the strike respectively. $I_c = \lim_{t^- \to t^+} \int_{t^-}^{t^+} f_n dt$ and $I_r = \lim_{t^- \to t^+} \int_{t^-}^{t^+} \tau_n dt$ are the impulses that act on the robot. Motion of the robot is constrained by the followed equation after the strike.

$$ \frac{\partial C_1}{\partial \boldsymbol{q}}\dot{\boldsymbol{q}}^+ = 0, \quad \frac{\partial C_2}{\partial \boldsymbol{q}}\dot{\boldsymbol{q}}^+ = 0 \tag{22} $$

Then, the equation of strike of matrix formation in the case of heel/tiptoe can be obtained from Eqs. (20)–(22).

$$ \begin{bmatrix} \boldsymbol{M}(\boldsymbol{q}) & -\boldsymbol{j}_c^T \\ \boldsymbol{j}_c & 0 \end{bmatrix} \begin{bmatrix} \dot{\boldsymbol{q}}^+ \\ I_c \end{bmatrix} = \begin{bmatrix} \boldsymbol{M}(\boldsymbol{q})\dot{\boldsymbol{q}}^- \\ 0 \end{bmatrix} \tag{23} $$

$$ \begin{bmatrix} \boldsymbol{M}(\boldsymbol{q}) & -\boldsymbol{j}_r^T \\ \boldsymbol{j}_r & 0 \end{bmatrix} \begin{bmatrix} \dot{\boldsymbol{q}}^+ \\ I_r \end{bmatrix} = \begin{bmatrix} \boldsymbol{M}(\boldsymbol{q})\dot{\boldsymbol{q}}^- \\ 0 \end{bmatrix} \tag{24} $$

3.4 Transition from (III) to (IV) and from (III′) to (IV)

When forefoot's slipping stops by friction force f_t, the phase (III) or (III′) is switched to (IV).

3.5 Transition from (IV) to (I)

This transition means that the tiptoe of the rear-foot (Link-6′) begins to detach from the ground in Phase (IV). If the value of constraint force f_n shown in Fig. 4 is positive, weight of the robot is supported by rear-leg. Therefore, the condition that rear-leg detaches from the ground is given as $f_n < 0$.

Table 1 Physical parameters of each link

Link Number	0	1	2	3	4
m_i [kg]	1.0	1.0	1.0	1.5	1.0
l_i [m]	0.5	2.0	2.0	1.5	2.0
r_i [m]	(1.0, 0.5)	0.2	0.2	0.2	0.2

Link Number	5	6	7	8
m_i [kg]	1.0	1.0	3.0	1.0
l_i [m]	2.0	0.5	2.0	0.5
r_i [m]	0.2	(0.5, 1.0)	0.2	0.5

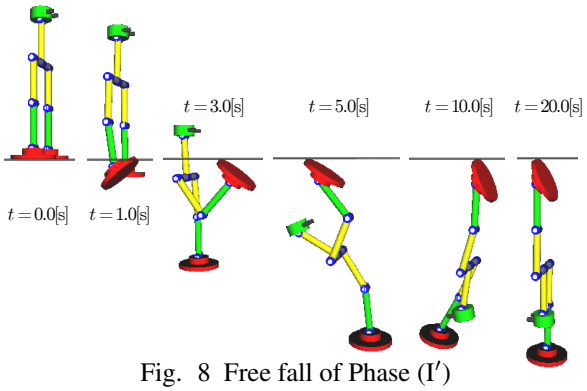

Fig. 8 Free fall of Phase (I′)

4. WALKING SIMULATION RESULT

As given condition of simulation, the robot's link has physical parameters listed in TABLE 1. We set all joint's coefficient of viscous friction as $d_i = 50.0$ [N·m·s/rad] ($i = 0, 1, \cdots, 7$), gravity acceleration as 9.8 [m/s^2] and sampling time as 0.002 [sec]. In regard to simulation environment, we used "Borland C++ Builder Professional Ver. 5.0" to compile simulation program and "OpenGL" to display humanoid robot's time-transient configurations.

4.1 Confirmation of dynamics and motion

This subsection verifies validity of the dynamics discussed in section 2. As a representative of non-constraint motion, free fall of Phase (I′) that is calculated under $\boldsymbol{\tau} = 0$ by Eq. (8) shown as Fig. 8. Figure 9 depicts free fall in Phase (III). This equation of motion is given by Eq. (17) that the foot being constraint by z-axis can move to y-axis by slipping.

4.2 Input torque

In order to keep a walking gait stable, feed-back control is generally useful. However we want to avoid to make a controller to generate stable gait motion by referring desired joint angles based on preferable body motion. Since this strategy has to keep a restriction of singularity of Jacobian matrix derived from inverse kinematical relation from body's desired velocity in world coordinates to joint angular velocity. Instead, a possibility for stable walking through Jacobian-transpose is examined in this paper. Simplifying and averting influences from a complex dynamics made by introducing feed-back controller, we had chosen a feed-forward input generated by a fixed and periodical time function.

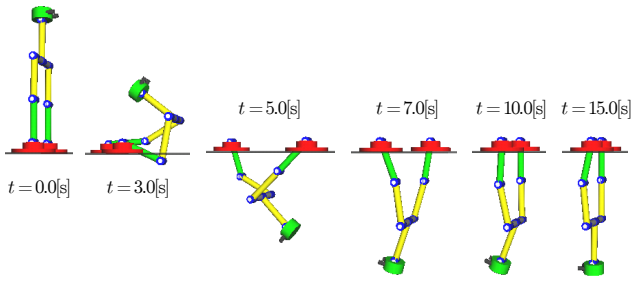

Fig. 9 Free fall of Phase (III) under $f_t = 0.0$

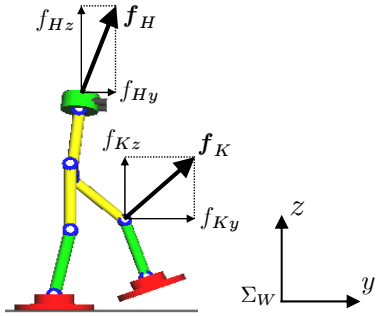

Fig. 10 Bipedal walking based on controlling a puppet

Inspired from controlling a puppet, suppose a two periodical forces $\boldsymbol{f}_K$ and $\boldsymbol{f}_H$ exert at head and lifting knee as shown Fig. 10, input torque $\boldsymbol{\tau}$ to generate walking strokes through $\boldsymbol{f}_K$ and $\boldsymbol{f}_H$ is given as:

$$\boldsymbol{\tau} = \boldsymbol{J}_K^T \boldsymbol{f}_K + \boldsymbol{J}_H^T \boldsymbol{f}_H. \tag{25}$$

In Eq. (25), $\boldsymbol{J}_K$ is Jacobian matrix from the the supporting foot to lifting knee, and $\boldsymbol{f}_K = [f_{Kx}, f_{Ky}, f_{Kz}]^T$ is force by which makes the knee step forward. Therefore, $\boldsymbol{f}_K$ is generated by rotating of Joint-0, 1, 2, 3 until floating foot attaches to the ground. On the other hand, $\boldsymbol{J}_H$ is Jacobian matrix from the supporting foot to the robot's head, and $\boldsymbol{f}_H = [f_{Hx}, f_{Hy}, f_{Hz}]^T$ is force pulling the robot's head up. $\boldsymbol{f}_H$ is always input by Joint-0, 1, 2, 6, 7, 8 to prevents head/body of the robot from dropping.

4.3 Example of bipedal walking

Under the environment that the relation of reaction force and friction force were represented as $f_t = 0.5 f_n$, this simulation was conducted. Joint's angular velocity was set as $\dot{\boldsymbol{q}}_i = \boldsymbol{0}$ ($i = 0, 1, \cdots, 8$) and the torque defined by Eq. (25) was input to each joint. Here,

$$\boldsymbol{f}_K = \begin{bmatrix} 0 \\ 4.0 \cos\left\{\frac{2.0\pi(t-T)}{2.9}\right\} \\ 40.0 \cos\left\{\frac{2.0\pi(t-T)}{2.9}\right\} \end{bmatrix}, \tag{26}$$

$$\boldsymbol{f}_H = [\,0,\ 0.49,\ 4.8\,]^T. \tag{27}$$

In Eq. (26), t means current time and T means the time spent for walking gait from Phase (IV) to next Phase (IV), meaning if previous Phase (IV) represents supporting leg is right, then next Phase (IV) shows left leg supports.

The robot walked in the sequences shown as Fig. 11 in this simulation. This figure means that although the

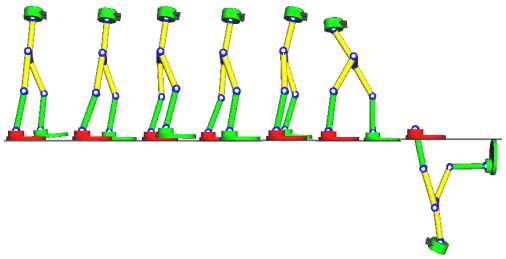

Fig. 11 Screenshot of walking simulation

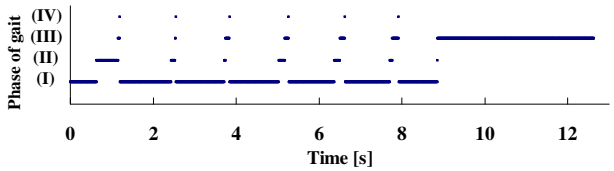

Fig. 12 Transition of gait

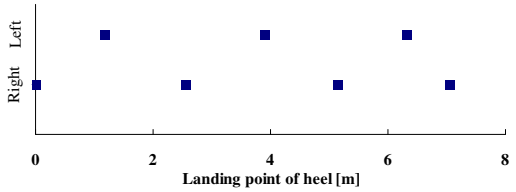

Fig. 13 Landing point of lifting heel

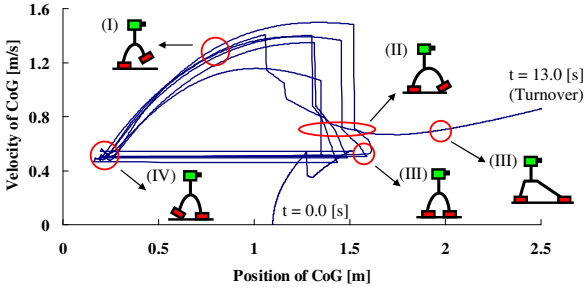

Fig. 14 Relation of walking cycle and gaits

robot could walk seven steps, the robot lost a balance and turned over since forefoot slipped greatly after that. Figures 12–14 describe gait's transition, landing position of lifting heel and relation the robot's position of center of gravity [CoG] and velocity of CoG relevant to traveling direction (y-axis in Σ_W).

5. CONCLUSION

In this paper, bipedal walking gait that contains slipping motion was divided into seven phase, and each dynamics whose dimension varies according to the state of supporting-foot was clearly derived through NE Method. Then, as results of some kinds of simulations, we verified that each dynamics was correctly calculated and appropriate gait was selected depending on motion of the robot. We confirmed that the robot walked some steps, slipped and turned over like human, which can express the human's gait with realistic.

REFERENCES

[1] M. Vukobratovic, A. Frank and D. Juricic, "On the Stability of Biped Locomotion," *IEEE Transactions on Biomedical Engineering*, Vol.17, No.1, 1970.

[2] M. Vukobratovic and J. Stepanenko, "On the Stability of Anthropomorphic Systems," *Mathematical Biosciences*, Vol.15, pp.1–37, 1972.

[3] K. Hirai, M. Hirose, Y. Haikawa and T. Takenaka, "The development of the Honda Humanoid robot," *Proc. IEEE International Conference on Robotics and Automation*, pp.1321–1326, 1998.

[4] S. Colins, A. Ruina, R. Tedrake and M. Wisse, "Efficient Bipedal Robots Based on Passive-Dynamic Walkers," *Science*, Vol.307, pp.1082–1085, 2005.

[5] J. Pratt, P. Dilworth and G. Pratt, "Virtual Model Control of a Bipedal Walking Robot," *Proc. IEEE International Conference on Robotics and Automation*", pp.193–198, 1997.

[6] R.E. Westervelt, W.J. Grizzle and E.D. Koditschek, "Hybrid Zero Dynamics of Planar Biped Walkers," *IEEE Transactions on Automatic Control*, Vol.48, No.1, pp.42–56, 2003.

[7] Y. Harada, J. Takahashi, D. Nenchev and D. Sato, "Limit Cycle Based Walk of a Powered 7DOF 3D Biped with Flat Feet," *Proc. of International Conference on IROS*, pp.3623–3628, 2010.

[8] S. Kajita, M. Morisawa, K, Miura, S. Nakaoka, K. Harada, K. Kaneko, F. Kanehiro and K. Yokoi, "Biped Walking Stabilization Based on Linear Inverted Pendulum Tracking," *Proc. IEEE/RSJ International Conference on Intelligent Robots and Systems*, pp.4489–4496, 2010.

[9] H. Dau, C. Chew and A. Poo, "Proposal of Augmented Linear Inverted Pendulum Model for Bipedal Gait Planning," *Proc. IEEE/RSJ International Conference on Intelligent Robots and Systems*, pp.172–177, 2010.

[10] S. Kajita and K. Tani, "Study of Dynamic Locomotion on Rigged Terrain-Derivation and Application of the Linear Inverted Pendulum Mode," *Proc. IEEE International Conference on Robotics and Automation*, pp.1405–1411, 1991.

[11] S. Kajita, F. Kanechiro, K. Kaneko, K. Yokoi and H. Hirukawa, "The 3D Linear Inverted Pendulum Mode: A simple modeling for a biped walking pattern generation," *Proc. IEEE/RSJ International Conference on Intelligent Robots and Systems*, 2001.

[12] J.H. Park and K.D. Kim, "Biped walking robot using gravity-compensated inverted pendulum mode and computed torque control," *Proc. IEEE International Conference on Robotics and Automation*, Vol.4, pp.3528–3593, 1998.

[13] P.B. Wieber, "Trajectory free linear model predictive control for stable walking in the presence of strong perturbations," *Proc. International Conference on Humanoid Robotics*, 2006.

[14] P.B. Wieber, "Viability and predictive control for safe locomotion," *Proc. IEEE/RSJ International Conference on Intelligent Robots and Systems*, 2008.

[15] A. Herdt, N. Perrin and P.B. Wieber, "Walking without thinking about it," *Proc. IEEE/RSJ International Conference on Intelligent Robots and Systems*, pp.190–195, 2010.

[16] Y. Huang, B. Chen, Q. Wang, K. Wei and L. Wang, "Energetic efficiency and stability of dynamic bipedal walking gaits with different step lengths," *Proc. IEEE/RSJ International Conference on Intelligent Robots and Systems*, pp.4077–4082, 2010.

[17] H. Hemami and B.F. Wyman, "Modeling and Control of Constrained Dynamic Systems with Application to Biped Locomotion in the Frontal Plane," *IEEE Trans. on Automatic Control*, AC-24-4, pp.526–535, 1979.

[18] C.L. Golliday and H. Hemami, "An Approach to Analyzing Biped Locomotion Dynamics and Designing Robot Locomotion Controls," *IEEE Trans. on Automatic Control*, AC-22-6, pp.963–972, 1997.

[19] Y. Nakamura and K. Yamane, "Dynamics of Kinematic Chains with Discontinuous Changes of Constraints—Application to Human Figures that Move in Contact with the Environments—," *Journal of RSJ*, Vol.18, No.3, pp.435–443, 2000 (in Japanese).

[20] J.Y.S. Luh, M.W. Walker and R.P.C. Paul, "On-Line Computational Scheme for Mechanical Manipulators," *ASME J. of DSME*, Vol.102, No.2, pp.69–76, 1980.

[21] M.W. Walker and D.E. Orin, "Efficient Dynamic Computer Simulation of Robotic Mechanisms," *ASME J. of DSME*, Vol.104, pp.205–211, 1982.